

# Semi-Empirical Fitting of Partial Pair Correlation Functions of Amorphous Alloys

E. Sváb, F. Hajdu, and Gy. Mészáros

Research Institute for Solid State Physics, 1525 Budapest POB 49, Hungary

Z. Naturforsch. **50a**, 1205–1210 (1995); received September 22, 1995

A semi-empirical fitting procedure has been developed and used in analysing the characteristic features of the partial structure factors of binary amorphous alloys. An analytical formula is given to fit the experimental atomic pair correlation function as a sum of Gaussians. The inverse Fourier transform of the fitted terms reproduces all features of the experimental structure function. In addition to the structural parameters, the modelling gives a quantitative explanation for the complex origin of characteristic features in the diffraction pattern such as pre-peak, pre-minimum, and split peaks in the partial structure factor.

**Key words:** Metallic glass, Short range order, Partial correlations, Neutron diffraction, Fitting.

## 1. Introduction

A semi-empirical fitting procedure was proposed in [1–3] as a means of characterizing the pair correlation function (PCF) and structure functions (SF) of liquids and amorphous solids in quantitative terms. However, the fitted parameters obtained gave characteristic structural figures such as coordination numbers, atom pair distances and their distribution widths only for one-component systems; for binary or more complex systems the fitted parameters were weighted averages of the corresponding partial quantities. In spite of these limitations, the method was successfully used in interpreting the measured X-ray data of liquid  $\text{H}_2\text{O}$  [1], glassy  $(\text{Fe, Ni})_{80}\text{B}_{20}$  [2–3], and some other amorphous alloys [4].

After having obtained reliable partial SFs and PCFs by isotopic neutron diffraction for several binary amorphous alloys (e.g. [5] and references therein) it became promising to apply the semi-empirical fit to partial functions of a binary alloy. The aim of this work was to adapt the fitting procedure to partial SFs and PCFs in order to characterize in quantitative terms the partial distributions and to clarify the origin of some special features of the partial structure functions, e.g. pre-peak, pre-minimum, shoulder of the second peak.

In the present paper the proposed fitting procedure is described in general, and its application to the ex-

perimental partial functions of amorphous  $\text{Ni}_{44}\text{Nb}_{56}$  [6] is presented in particular.

## 2. Modelling Procedure

The fitting procedure is based on the experimental partial pair correlation functions,  $g_{ab}(r)$ . They are approximated by a series of modified Gaussian functions. Before subjected to fitting,  $g_{ab}(r)$  are slightly smoothed in the following way:

- the experimental spurious oscillations in the range between zero and the first real peak are removed;
- the  $r$ -range is finished with some arbitrariness at a certain  $R_c$  ( $\approx 1.5$ – $2$  nm), so that each  $g_{ab}(r)$  becomes 1 for  $r > R_c$ . With this smoothing we set a limit to the number of fitted parameters and let the convergence of  $g_{ab}(r) - 1$  be perfect. For the sake of a minimum “cut-off” effect,  $R_c$  itself is also a fitted parameter.

The fitted analytical expression of a PCF consists of three terms. For simplicity we omit the notation of “ab”:

$$g(r) = g_d(r) + g_c(r) + g_t(r), \quad (1)$$

where

$$g_d(r) = \sum_{i=1}^p \frac{K_i}{\sqrt{32\pi^3} \varrho_0 R_i b_i r} \left[ \exp\left(-\frac{(r-R_i)^2}{2b_i^2}\right) - \exp\left(-\frac{(r+R_i)^2}{2b_i^2}\right) \right], \quad (2)$$

Reprint requests to Dr. E. Sváb.

0932-0784 / 95 / 1200-1205 \$ 06.00 © – Verlag der Zeitschrift für Naturforschung, D-72027 Tübingen



Dieses Werk wurde im Jahr 2013 vom Verlag Zeitschrift für Naturforschung in Zusammenarbeit mit der Max-Planck-Gesellschaft zur Förderung der Wissenschaften e.V. digitalisiert und unter folgender Lizenz veröffentlicht: Creative Commons Namensnennung-Keine Bearbeitung 3.0 Deutschland Lizenz.

Zum 01.01.2015 ist eine Anpassung der Lizenzbedingungen (Entfall der Creative Commons Lizenzbedingung „Keine Bearbeitung“) beabsichtigt, um eine Nachnutzung auch im Rahmen zukünftiger wissenschaftlicher Nutzungsformen zu ermöglichen.

This work has been digitalized and published in 2013 by Verlag Zeitschrift für Naturforschung in cooperation with the Max Planck Society for the Advancement of Science under a Creative Commons Attribution-NoDerivs 3.0 Germany License.

On 01.01.2015 it is planned to change the License Conditions (the removal of the Creative Commons License condition “no derivative works”). This is to allow reuse in the area of future scientific usage.

$$g_c(r) = 0 \quad \text{for } r < R_c; \quad g_c(r) = 1 \quad \text{for } r \geq R_c, \quad (3)$$

$$g_t(r) = \frac{R_c}{r} \exp\left(-\frac{(R_c - r)^2}{2b_c^2}\right) \quad \text{for } r < R_c; \\ g_t(r) = 0 \quad \text{for } r \geq R_c. \quad (4)$$

The main part of the approximating formula (1) is  $g_d(r)$ . It consists of slightly modified Gaussian functions, centred around increasing  $R_i$  positions. The  $R_i$  are the radii of concentric coordination spheres surrounding any atom chosen arbitrarily as the origin. Apart from the mean radius  $R_i$ , the  $i$ -th Gaussian term ( $i=1, 2, \dots, p$ ) contains two additional variable parameters, viz.  $b_i$ , the root mean square deviation of the pair distances around  $R_i$ , and  $K_i$ , the number of atoms in this sphere. The approximating formula for PCFs is closed by two further terms; a step function  $g_c(r)$  is zero below  $R_c$  and equals 1 above it (see (3)); and a truncated modified Gaussian function  $g_t(r)$  is shifted with its maximum to  $r=R_c$ , where it jumps to zero (see (4)). These two functions, added to the series of Gaussians, yield a smooth transition to  $g_{ab}(r)=1$  in the high  $r$ -range.

In the course of computing we found that a slight modification of the experimental partial PCF improved the resolution of peaks, and so it became more suitable for being approximated with Gaussians. We have used the expression

$$g_{ab}^*(r) = \frac{G_{ab}(r)}{4\pi r \varrho_0 \sqrt{c_a c_b}} + 1 \quad (5)$$

instead of  $g_{ab}(r)$  introduced in the literature as (see e.g. [7])

$$g_{ab}(r) = \frac{G_{ab}(r)}{4\pi r \varrho_0} + 1, \quad (6)$$

where  $G_{ab}(r)$  is the reduced distribution function obtained by Fourier transformation from the corresponding partial SF. The only physical consequence of the modified  $g_{ab}^*(r)$  formula is that the coordination numbers  $K_{ab}$  obtained by the approximation cannot be taken as exactly equal to the  $Z_{ab}$  experimental ones [6]. The following relationship holds for them:

$$Z_{ab} = c_b \sqrt{c_a c_b} K_{ab} + 4\pi \varrho_0 c_b (1 - \sqrt{c_a c_b}) \frac{r_2^3 - r_1^3}{3}. \quad (7)$$

where  $r_1$  and  $r_2$  are the limits of the integral in  $\text{RDF}_{ab}(r)$  when calculating  $Z_{ab}$ . Obviously, the multiplication factor of  $K_{ab}$  is smaller than 1, thus it dimin-

ishes  $K_{ab}$ ; the second term, however, is always positive, and so it increases the sum. Accordingly, the corrections partly or entirely cancel each other, thereby  $K_{ab} \sim Z_{ab}$ . We note that a slight deviation may be due to the different procedures in separating neighbouring coordination shells.

Once the partial PCF has been obtained as an analytical expression containing the fitted numerical parameters, it can be Fourier transformed to get the partial SF. The simulated structure factor  $S(Q)$  is composed of three terms in correspondence with (1–4):

$$S(Q) = S_d(Q) + S_c(Q) + S_t(Q), \quad (8)$$

$$S_d(Q) = \sum_{i=1}^p K_i \exp\left(-\frac{b_i^2 Q^2}{2}\right) \frac{\sin(R_i Q)}{R_i Q}, \quad (9)$$

$$S_c(Q) = \frac{4\pi \varrho_0}{Q^3} [R_c Q \cos(R_c Q) - \sin(R_c Q)], \quad (10)$$

$$S_t(Q) = 4\pi \varrho_0 R_c b_c \exp\left(-\frac{b_c^2 Q^2}{2}\right) \cdot \left[ \sqrt{\frac{\pi}{2}} \sin(R_c Q) - b_c Q \cos(R_c Q) \Phi(Q) \right] \quad (11)$$

with

$$\Phi(Q) = \sum_{n=0}^{\infty} \frac{1}{(2n+1)n!} \left(\frac{b_c^2 Q^2}{2}\right)^n. \quad (12)$$

The separate terms of the  $S_d(Q)$  function appear as damped sinusoid waves of different wavelengths inversely proportional to  $R_i$ . The initial amplitude is proportional to  $K_i$ , and the damping factor depends exponentially on  $-b_i^2$ . The superposition of such waves makes up the major part of the structure factor.

It must be noted that the integrand of the Fourier integral is not  $g(r)$  itself but  $4\pi \varrho_0 r [g(r) - 1]$ . The subtrahend 1 and the factor  $4\pi \varrho_0 r$  must be accounted for in determining the Fourier transform. Subtracting 1 is best to be performed in the step function  $g_c(r)$ , which is then  $-1$  for  $0 < r < R_c$  and 0 for  $r \geq R_c$ . This function has to be multiplied by  $4\pi \varrho_0 r$ . Its sine-Fourier transform is a Bessel function of first order (see (10)). The transform of the truncated Gaussian can also be expressed in analytical form (see (11)). Similarly to (10) it contains a term with  $\sin(R_c Q)$  and another with  $\cos(R_c Q)$ , however with opposite signs (i.e. a phase shift of  $180^\circ$ ) and different coefficients. Both of these transforms are strongly oscillating and slowly damping periodic functions of  $Q$ , the period length being inversely proportional to  $R_c$ . The sum of  $S_c(Q)$  and  $S_t(Q)$  results in a moderately oscillating function with

apparent damping in the low  $Q$ -range, and it is zero for higher  $Q$ -values where the oscillations cancel each other completely. In the low  $Q$ -range between 0 and the first main maximum of  $S(Q)$  the oscillations of the three functions in (9–11) cancel each other and result in a smooth behaviour. In some cases, however, cancellation is not perfect and a peak appears in this region. This peak corresponds to the experimentally obtained pre-peak.

By the present method we can simulate the structure function in the form of a few superimposed periodic functions of the variable  $Q$ , where each function represents the contribution of atoms in a certain coordination shell except the last term, which originates from the atoms lying beyond the short range order limit. The effect of each atomic coordination shell on the coherent scattering is separated in this way, and the correlations between various features of the structure function and the characteristics of the atomic short range order can be studied.

The following remarks should be made on the accuracy of the fit. Apart from the positions of sharp peaks, the values of fitted parameters are not well defined. A reason for this is that the expansion of a function in Gaussians is not unambiguous. However, the fit can be checked by its standard deviation

$$\sigma = \left[ \frac{\sum_{j=1}^n [g_{\text{fit}}(r_j) - g_{\text{meas}}(r_j)]^2}{n-1} \right]^{\frac{1}{2}}, \quad (13)$$

where  $g_{\text{fit}}(r)$  and  $g_{\text{meas}}(r)$  denote the model and the measured PCF  $r_j (1 \leq j \leq n)$  are the discrete arguments where  $g_{\text{fit}}(r)$  and  $g_{\text{meas}}(r)$  are known.

Another check of the fit is based on the sum-rule related to the number of atoms  $N$  within the sphere of radius  $R_c$ . In principle the following equation should be valid:

$$\sum_{i=1}^p K_i + 4\pi\varrho_0 R_c b_c \left( \sqrt{\frac{\pi}{2}} R_c - b_c \right) = \frac{4\pi}{3} \varrho_0 R_c^3 - 1, \quad (14)$$

where the first term on the left hand side means the total number of discrete neighbours, and the second term is the area under the terminating halved Gaussian defined in (4). The right hand side is the total number of atoms in the same sphere as calculated from the mean atomic density  $\varrho_0$  diminishing by the central atom. Any difference found between the numerical values of the left and right hand sides of (14) represents  $\Delta N$ , which can be used as a measure of accuracy of the fit.

### 3. Results for Amorphous $\text{Ni}_{44}\text{Nb}_{56}$

The semi-empirical fitting procedure was performed on the partial PCFs and SFs of amorphous  $\text{Ni}_{44}\text{Nb}_{56}$  [6] investigated by the isotopic neutron diffraction method. Figure 1 shows the experimental  $g_{\text{NiNi}}^*(r)$ ,  $g_{\text{NiNb}}^*(r)$  and  $g_{\text{NbNb}}^*(r)$  function, the fitted Gaussian terms, and the sum of the Gaussians denoted as fitted partial PCF in the range  $0 \leq r \leq R_c$ . Each parameter set comprises 8 or 10 discrete distances  $R_i$  and the corresponding  $K_i$  and  $b_i$  parameters. In addition to these parameters, the terminating distance  $R_c$  at about  $1.8\text{--}2\text{ nm}^{-1}$  and its root mean square deviation  $b_c$  are also obtained by fitting.

Practically all characteristic features are reproduced. In the partial Ni–Ni and Nb–Nb distributions

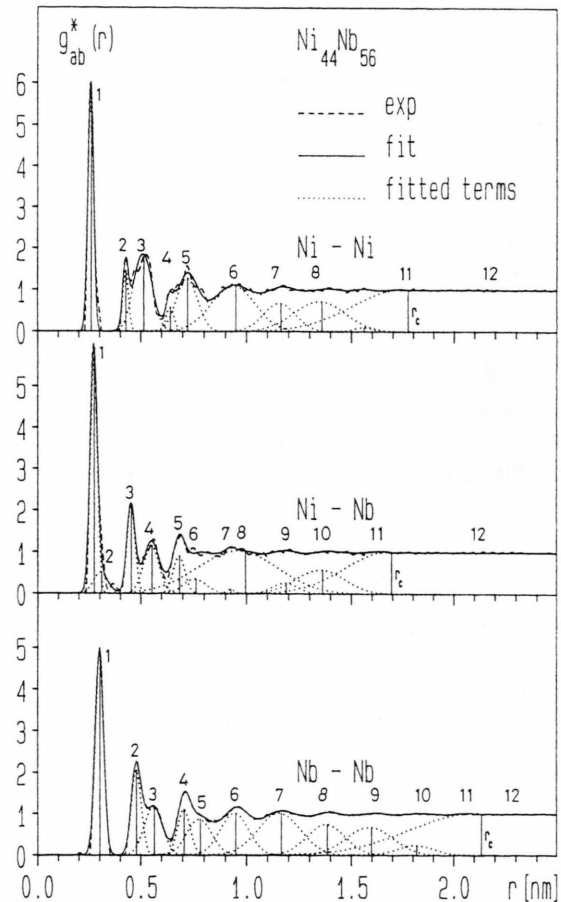


Fig. 1. Partial Ni–Ni, Ni–Nb and Nb–Nb pair correlation functions of amorphous  $\text{Ni}_{44}\text{Nb}_{56}$ : experimental (dashed line), fitted Gaussians of (1–4) (dotted lines) and the sum of these denoted fitted PCF (solid line).

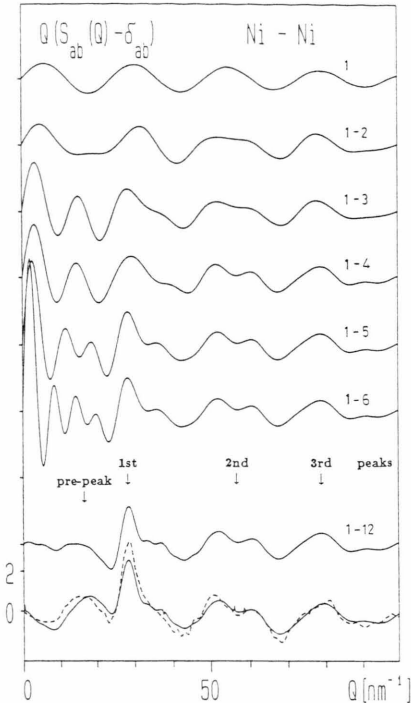


Fig. 2. Ni–Ni partial structure factor of amorphous  $\text{Ni}_{44}\text{Nb}_{56}$ : computed curves (solid lines, denoted by 1– $n$ ) represent the sum of the first  $n$  contributions of the fitting procedure. The experimental structure factor (dashed line) is compared with the final results of the computation.

approximately 7 fitted functions (up to 1.2 nm) can be distinguished as atomic subshells. In the case of Ni–Nb the fit is poorer, the broad Gaussian centered at 0.985 nm overlaps with others in the range above 0.6 nm. The corresponding parameters of the fitted functions for the three first coordination shells are collected in Table 1.

As a next step of the fitting procedure, the three partial SFs are calculated using the fitted parameters according to (8–12). The contributions of subsequent separate terms of (9–11), added to the sum of the previous ones are shown in Figs. 2–4 for Ni–Ni, Ni–Nb and Nb–Nb partial SFs, respectively. Thus, the first six curves represent the contributions of the first six fitted functions, where the curve denoted by 1– $n$  is the sum of the first  $n$  contributions. The seventh curve depicts the sum of all terms including the Fourier transform of the truncated Gaussian and that of the closing step function. In order to compare the calculated SF with the experimental curve, one has still to take into consideration the effect of the inverse

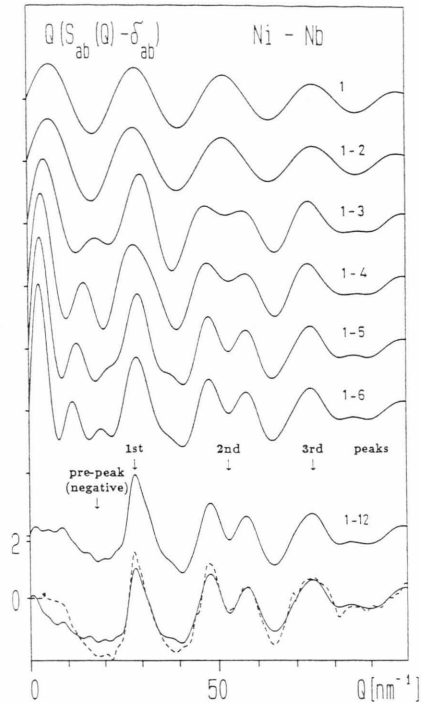


Fig. 3. Ni–Nb partial structure factor of amorphous  $\text{Ni}_{44}\text{Nb}_{56}$ : computed curves (solid lines denoted by 1– $n$ ) represent the sum of the first  $n$  contributions of the fitting procedure. The experimental structure factor (dashed line) is compared with the final result of the computation.

Table 1. Structural parameters for the three first coordination spheres in amorphous  $\text{Ni}_{44}\text{Nb}_{56}$  obtained by semi-empirical modelling of the experimental partial pair correlation functions.

Coord. sphere	Ni–Ni			Ni–Nb			Nb–Nb		
	$R_i$ [nm]	$b_i$ [nm]	$Z_i$ [atom]	$R_i$ [nm]	$b_i$ [nm]	$Z_i$ [atom]	$R_i$ [nm]	$b_i$ [nm]	$Z_i$ [atom]
1	0.258	0.013	3.71	0.272	0.017	5.70	0.301	0.021	8.29
				0.309	0.035	5.48			
2	0.427	0.014	5.37	0.454	0.020	13.00	0.480	0.024	10.60
	0.514	0.044	15.04	0.552	0.038	15.08	0.564	0.043	19.75
3	0.642	0.018	7.54	0.683	*	*	0.707	0.030	18.70
	0.724	0.050	20.49	0.762	*	*	0.782	0.058	29.20

\* The amplitude and half width value of the fitted Gaussian has no physical meaning because of a broad overlapping fitted Gaussian centred at 0.985 nm.

FT of the formerly omitted experimental spurious oscillations in the range between zero and the first real peak in  $g_{ab}^*(r)$ . As final curve, it is drawn together with the corresponding experimental structure factor.

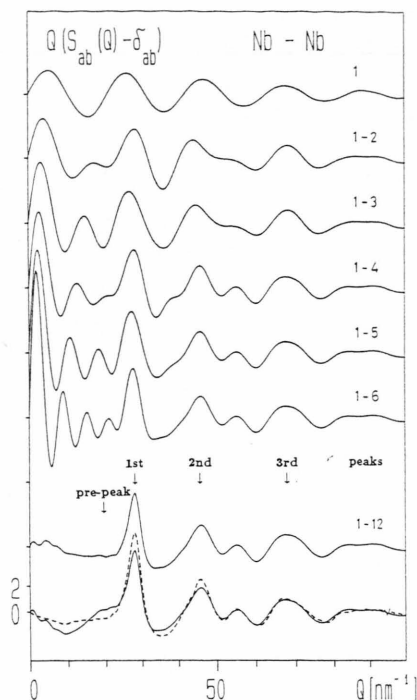


Fig. 4. Nb–Nb partial structure factor of amorphous  $\text{Ni}_{44}\text{Nb}_{56}$ : computed curves (solid lines denoted by 1– $n$ ) represent the sum of the first  $n$  contribution of the fitting procedures. The experimental structure factor (dashed line) is compared with the final result of the computation.

The semi-empirical computed partial SFs explicitly show the contributions of all discrete pair distances, and that of the range of continuously dispersed pairs also. The origin of various features of the experimental partial SF can be analysed as interference effects among atom pairs. Practically all features of the experimental  $S(Q)$  functions could be reproduced in the way outlined above. This gives an insight into the “mechanism” of how some special features in the SF arise.

The curves give evidence for the following statements:

- the profile of the 1st main peak is formed by the contribution of atoms distributed up to the 5th coordination shell. On adding the contribution of further neighbours, practically no changes occur in the peak positions, peak widths and the fine details

including the sub-peak in the Ni–Ni or the small hump in the Ni–Nb structure factors;

- the characteristic features of the 2nd peak, namely splitting up into two subpeaks, are determined mainly by atomic neighbours up to the 4th coordination shell. For the Ni–Ni and Nb–Nb SFs where the split is not very sharp, further neighbours do not play any role. However, in the final formation of the two well separated subpeaks in the Ni–Nb structure factor two subsequent atomic coordination shells contribute as well;
- the 3rd peak is determined mainly by neighbouring atoms up to the 2nd coordination shell;
- the pre-peak region is formed by all atomic pair distributions up to a medium range of about 1.8 nm. However the contribution of the high  $r$ -side subshell in the second coordination sphere (denoted as 3rd Gaussian for Ni–Ni and Nb–Nb, whereas 4th for Ni–Nb) is dominant at this position. Its relative intensity ratio to the first coordination sphere, which has a minimum value in this region, determines the final hump (maximum or minimum) at the  $Q$ -range between zero and the first main diffraction peak. The partial structure factor for Ni–Ni pairs exhibits a pre-peak around  $19 \text{ nm}^{-1}$ , for Nb–Nb shows up a shoulder at  $20 \text{ nm}^{-1}$  and for Ni–Nb a pre-minimum around  $20 \text{ nm}^{-1}$ . We refer here to [6], where the appearance of pre-peaks was correlated with the packing densities of the first and second coordination shells. This finding is now supported.

#### 4. Conclusions

As a result of this fitting procedure the following points are emphasized:

- an analytical formula may be used in theoretical calculations to replace the empirical numerical partial PCF functions;
- structural parameters, i.e. preferred radial distances, their distribution widths and their coordination numbers may be refined;
- the effect of each term on the formation of a partial SF can be analysed, and its special features may be related to the contribution of certain atomic coordination shells.

- [1] F. Hajdu, *Acta Chim. Hung.* **93**, 371 (1977).
- [2] F. Hajdu, *Phys. Status Solidi(a)* **60**, 365 (1980).
- [3] F. Hajdu, *ibid.* **61**, 141 (1980).
- [4] G. Cocco, S. Enzo, M. Sampoli, and L. Schiffrini, *J. Non-Cryst. Solids* **61&62**, 577 (1984).
- [5] S. Steeb and P. Lamparter, *J. Non-Cryst. Solids* **156–158**, 24 (1993).
- [6] E. Sváb, Gy. Mészáros, J. Takács, S. N. Ishmaev, S. I. Isakov, and I. P. Sadikov, *J. Non-Cryst. Solids* **144**, 99 (1992).
- [7] Y. Waseda, *The Structure of Non-Crystalline Materials*, McGraw-Hill, New York 1980.